Title	Calibrated CFD simulation to evaluate thermal comfort in a highly-glazed naturally ventilated room
Author(s)	Hajdukiewicz, Magdalena; Geron, Marco; Keane, Marcus M.
Publication Date	2013-08-30
Publication Information	Hajdukiewicz, Magdalena, Geron, Marco, & Keane, Marcus M. (2013). Calibrated CFD simulation to evaluate thermal comfort in a highly-glazed naturally ventilated room. Building and Environment, 70, 73-89. doi: http://dx.doi.org/10.1016/j.buildenv.2013.08.020
Publisher	Elsevier
Link to publisher's version	http://dx.doi.org/10.1016/j.buildenv.2013.08.020
Item record	http://hdl.handle.net/10379/6176
DOI	http://dx.doi.org/10.1016/j.buildenv.2013.08.020

Calibrated CFD simulation to evaluate thermal comfort in a highly-glazed naturally ventilated room.

Ms. Magdalena Hajdukiewicz [a,b,c]

Dr. Marco Geron [a,b,c]

Dr. Marcus M. Keane [a,b,c]

[a] *Informatics Research Unit for Sustainable Engineering (IRUSE) Galway, Ireland*

[b] *Department of Civil Engineering, National University of Ireland Galway, Galway, Ireland*

[c] *Ryan Institute, National University of Ireland Galway, Galway, Ireland*

Corresponding author: *Magdalena Hajdukiewicz*

Department of Civil Engineering, National University of Ireland Galway, Galway, Ireland

E-mail: m.hajdukiewicz1@nuigalway.ie

Phone: +353 (0) 91 49 33 58

Fax: +353 (0) 91 49 45 07

Please reference as:
Hajdukiewicz, M., Geron, M., & Keane, M.M., 2013. 'Calibrated CFD simulation to evaluate thermal comfort in a highly-glazed naturally ventilated room'. *Building and Environment*, 70, pp. 73-89. http://dx.doi.org/10.1016/j.buildenv.2013.08.020

Abstract

Natural ventilation is a sustainable solution to maintaining healthy and comfortable environmental conditions in buildings. However, the effective design, construction and operation of naturally ventilated buildings require a good understanding of complex airflow patterns caused by the buoyancy and wind effects.

The work presented in this article employed a 3D computational fluid dynamics (CFD) analysis in order to investigate environmental conditions and thermal comfort of the occupants of a highly-glazed naturally ventilated meeting room. This analysis was facilitated by the real-time field measurements performed in an operating building, and previously developed formal calibration methodology for reliable CFD models of indoor environments. Since, creating an accurate CFD model of an occupied space in a real-life scenario requires a high level of CFD expertise, trusted experimental data and an ability to interpret model input parameters; the calibration methodology guided towards a robust and reliable CFD model of the indoor environment. This calibrated CFD model was then used to investigate indoor environmental conditions and to evaluate thermal comfort indices for the occupants of the room. Thermal comfort expresses occupants' satisfaction with thermal environment in buildings by defining the range of indoor thermal environmental conditions acceptable to a majority of occupants. In this study, the thermal comfort analysis, supported by both field measurements and CFD simulation results, confirmed a satisfactory and optimal room operation in terms of thermal environment for the investigated real-life scenario.

Keywords

CFD; measurement; indoor environment; natural ventilation; calibration; thermal comfort

1. Introduction

People spend on average 90% of their lives indoors [1]. All aspects of human life, from working, sleeping and studying, to taking part in leisure activities occur indoors. Thus, it is vital to provide safe, healthy and comfortable conditions in buildings. The building sector is responsible for 40% of the total energy consumption and 36% of total CO2 emissions in the European Union [2]. Up to a half of the energy consumed by buildings is due to the use of heating, ventilation and air conditioning (HVAC) systems [3].

Well-designed building ventilation systems supply fresh and remove stale air, in order to provide satisfactory indoor air quality for building occupants [4]. At the same time, ventilation systems have an impact on the occupants' comfort, e.g. through temperature differences or excessive air movement. Thus, during building design and operation it should be intended to provide adequate ventilation, while reducing building energy use and maximising occupants comfort at the same time [4].

Natural ventilation is increasingly seen as a sustainable solution to maintaining healthy and comfortable environmental conditions in buildings. In natural ventilation systems the airflow is driven through ventilation openings by the natural driving forces of wind (wind effect) and temperature

Please reference as:
Hajdukiewicz, M., Geron, M., & Keane, M.M., 2013. 'Calibrated CFD simulation to evaluate thermal comfort in a highly-glazed naturally ventilated room'. *Building and Environment*, 70, pp. 73-89. http://dx.doi.org/10.1016/j.buildenv.2013.08.020

(buoyancy effect). Although, natural ventilation has a great potential in reducing buildings energy consumption (for ventilation and cooling purposes), it meets many barriers before it can be implemented. Natural ventilation is often considered too risky, due to a perceived lack of ability to predict and control its effects [5]. An effective design of a naturally ventilated space requires a good understanding of complex airflow patterns caused by buoyancy and wind effects. Thus, without adequate tools to predict and optimise environments in naturally ventilated buildings, the provision of healthy and comfortable conditions for occupants cannot be guaranteed with any degree of confidence. There are no 'off-the-shelf' solutions for natural ventilation. Designers must consider many factors when proposing natural ventilation; many of these factors are not as critical in mechanically ventilated buildings (e.g. restrictions regarding outdoor conditions, such as location, wind patterns, air quality, noise, etc.) [6].

At the design stage, architects often do not consider natural ventilation solutions due to the lack of expertise to implement it. Furthermore, where natural ventilation is successfully employed in the design, there is a risk of harming the project during the construction stage. This may be caused by contractors who do not fully realise or understand natural ventilation and make unilateral changes that can significantly affect the system [7]. Thus, this lack of knowledge in the industry may result in poorly designed, constructed and operated naturally ventilated buildings.

There exists a significant challenge to create the quality simulation models that predict the performance of naturally ventilated spaces and show compliance with environmental requirements. There is a need for simulation tools that can enable acceptable thermal performance of naturally ventilated buildings, through the design and optimisation stages [8]. The industry expressed a desire for new design tools on natural ventilation, including calculation rules and easy to use, simple and advanced computer programmes [5].

2. Objectives

For the last 50 years CFD has become progressively more popular and accessible for research and industry sectors, mainly because of the development and advancement in computing processing power and the availability of commercial software. The ability to deal with complex flows within built environments has made CFD an important tool in improving building health and safety ([9], [10]); ensuring thermal comfort for the occupants ([11], [12]); testing energy efficient designs ([13], [14]); and applying required environmental conditions ([15], [16]).

CFD is a powerful numerical simulation tool. However, the accuracy and reliability of CFD predictions remains a major concern (e.g. Refs. [17] - [19]). The accuracy of CFD results depends on the modeller's knowledge in fluid dynamics, the expertise to handle complex boundary conditions and skills in numerical techniques (e.g. Refs. [20] - [22]). Many types of errors may occur in a CFD simulation (i.e. discretisation, round-off, iteration, physical modelling or human errors). In order to obtain credible results, a systematic procedure for model generation should be followed.

Motivated by the lack of systematic methods for creating reliable CFD models of naturally ventilated indoor environments, the authors of this paper previously developed a formal calibration methodology

Please reference as:
Hajdukiewicz, M., Geron, M., & Keane, M.M., 2013. 'Calibrated CFD simulation to evaluate thermal comfort in a highly-glazed naturally ventilated room'. *Building and Environment*, 70, pp. 73-89. http://dx.doi.org/10.1016/j.buildenv.2013.08.020

for CFD models relating to naturally ventilated spaces [23]. The methodology explains how to qualitatively and quantitatively verify and validate CFD model utilising field measurements; as well as, perform parametric analysis to support a robust calibration process. Applying the methodology optimises the decision making process when creating a final valid CFD model of a naturally ventilated space. Developed concepts and techniques recognise the practical modelling of occupied spaces in real-life environments. Furthermore, those concepts and techniques enhance the process of achieving reliable CFD models that represent indoor spaces, and provide new and valuable information about the effects of numerical boundary conditions on CFD model results when modelling indoor environments.

This article presents the application of a calibrated CFD model of a highly-glazed naturally ventilated meeting room. The model calibration process was supported by the calibration methodology and field measurements in an operating building. The calibrated CFD model was then used to investigate indoor environmental conditions and evaluate thermal comfort indices for the room occupants. A satisfactory and optimal room operation in terms of the thermal environment for the investigated real-life scenario was confirmed.

3. Methodology

This paper investigates environmental conditions and thermal comfort of the occupants of a naturally ventilated room. This investigation was facilitated by the real-time field measurements in the operating building and the formal calibration methodology for reliable and robust CFD models of indoor environments [23]. The calibration methodology (Figure 1) explains how to verify and validate a CFD model, and perform parametric analysis to evaluate the influence of model boundary conditions on simulation results. The outcome of the calibration procedure is a reliable CFD model that, based on the field measurements, accurately represents operating indoor environment.

Figure 1. Formal calibration methodology relating to CFD models of indoor environments [23].

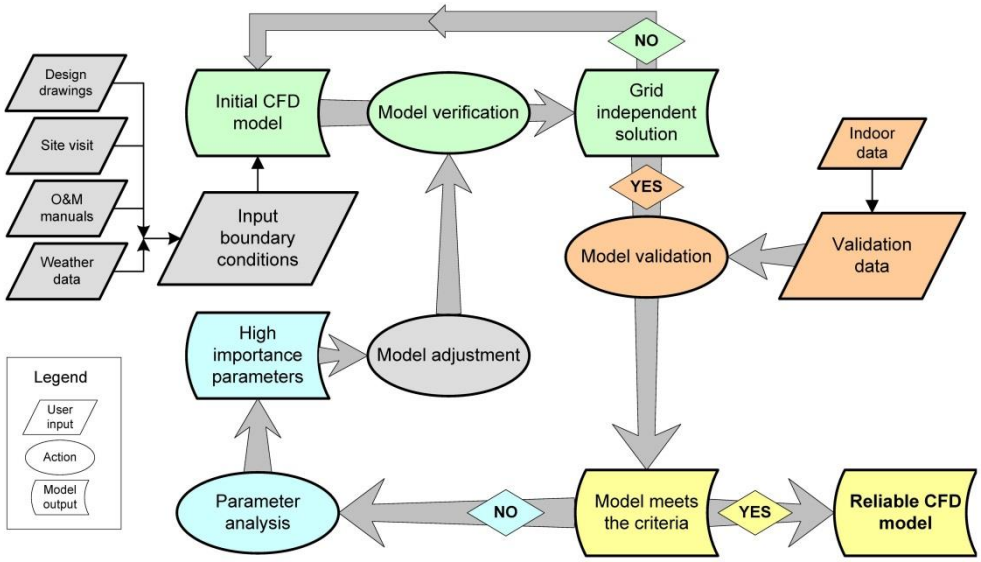

Please reference as:
Hajdukiewicz, M., Geron, M., & Keane, M.M., 2013. 'Calibrated CFD simulation to evaluate thermal comfort in a highly-glazed naturally ventilated room'. *Building and Environment*, 70, pp. 73-89. http://dx.doi.org/10.1016/j.buildenv.2013.08.020

Based on the technical documentation, site visits and on-site measurements the initial CFD model of the indoor space is created. Following this, a grid verification study takes place. Various runs of the initial CFD model are performed on different size meshes and their results are compared to analyse the grid independence of the solution. A grid independent solution implies the results do not change significantly with increasing number of mesh cells, i.e. the balance between accuracy and computational time is achieved. In this research work, the grid independent solution is quantitatively evaluated using the *GCI* method introduced by Roache [24]. Once the grid independence is established, the simulated air speeds and air temperatures inside the internal space are validated with on-site measurements. A validation process should be performed using available reliable data, in order to prove the ability of the CFD model to predict indoor conditions [25]. Generally, validation criteria depend on the modelled environment (e.g. office spaces require thermal comfort of the occupants, while data centres or clean rooms demand rigorous indoor conditions) and errors/uncertainties in measured and simulated data. This work investigates environmental conditions in a meeting room occupied by people. Thus, the validation criteria are determined based on the requirements of occupants' comfort and measurement uncertainties. When the model meets the specified validation criteria, it is regarded as a true representation of the real environment. If the criteria are not met, a parametric analysis is performed. Parametric analysis allows for the determination of the boundary conditions that most influence model output results. The next step is the process of improving the agreement between experimental and simulated data by adjusting the most relevant input parameters. This step should be repeated as long as the CFD model meets the validation criteria of being a good representation of the real environment.

4. Demonstrator

4.1. Overview of the building

The demonstrator used in this work is the Engineering Building at the National University of Ireland (NUI) Galway, Ireland (Figure 2a). With a gross floor area of 14 100 m^2, the Engineering Building is the largest school of engineering in Ireland. This building was opened to public in September 2011. The Engineering Building was designed as a 'living laboratory' in order to provide real-time measured data of structural and environmental building performance [26].

Figure 2. Engineering Building at the NUI Galway (a) and modelled meeting room (b).

a

Please reference as:
Hajdukiewicz, M., Geron, M., & Keane, M.M., 2013. 'Calibrated CFD simulation to evaluate thermal comfort in a highly-glazed naturally ventilated room'. *Building and Environment*, 70, pp. 73-89. http://dx.doi.org/10.1016/j.buildenv.2013.08.020

b 

A naturally ventilated meeting room (Figure 2b) on the top floor of the Engineering Building was chosen in order to study indoor environmental conditions. The dimensions of the room are 4.90 m (D) x 5.89 m (L) x 3.47 m (H). The room is cross-ventilated with two external walls consisting of windows (facing north and east directions). The internal wall facing west direction is a concrete structural wall adjacent to the internal staircase. The second internal wall facing south direction is a partition wall adjacent to an office space. During the experiment, the air entered the room through the window awning inlet (facing east direction) and exited through the window awning outlet (facing north direction). The dimensions of both the inlet and outlet were 0.27m x 1.31m.

4.2. Field measurements

4.2.1. Outdoor measurements

The measurement of outdoor weather conditions was facilitated by the automatic weather station [27] located at the NUI Galway campus [28]. The station was installed according to the best practice guidelines regarding its location in July 2010 on the roof of one of the University buildings (in the centre of the campus, in an open space without any tall buildings in its proximity), approximately 500 m from the Engineering Building. The weather station measures dry-bulb air temperature (oC) and relative humidity (%), barometric pressure (mBar), wind speed (m/s) and wind direction (o), global and diffuse solar irradiance (W/m2), and rainfall (mm). The measurements are taken with a time step of 1 minute (except the rainfall, for which it is 1 hour).

The weather station provides essential data to support the development and calibration of computational models (CFD, whole building simulation and reduced order models) at the NUI Galway. Moreover, the weather station gives a reliable overview of the weather conditions in Galway. Finally, the live and historical weather data measured by the station can be accessed by general public online [28] or by using a smart phone application [29].

4.2.2. Indoor measurements

For the CFD model validation purposes indoor air temperatures were measured using a network of fourteen wireless Hobo U12 data loggers (denoted by the letter S) [30]. Those data loggers were located in four horizontal layers (ankles level (h = 0.1 m), sitting person's waist level (h = 0.6 m), sitting person's head level (h = 1.1 m) and standing person's head level (h = 1.7 m)) in order to observe the air temperature stratification inside the room that affected occupants' thermal comfort.

Please reference as:
Hajdukiewicz, M., Geron, M., & Keane, M.M., 2013. 'Calibrated CFD simulation to evaluate thermal comfort in a highly-glazed naturally ventilated room'. *Building and Environment*, 70, pp. 73-89. http://dx.doi.org/10.1016/j.buildenv.2013.08.020

Moreover, three Egg-Whisk sensors (denoted by letters EW) [31] were used to measure air speeds inside the room. The Egg-Whisk sensing platforms are based on the Tyndall [32] modular prototyping mote [33] and were specifically designed to obtain a comprehensive record of the environmental conditions (such as air temperature, relative humidity, air speed, CO2 concentration, ambient lighting levels, sensor movement and noise) at various spatiotemporal points within an indoor space.

The measurement setup for air temperature and air speed sensors inside the room is presented in Figure 3. Two air speed sensors [30] located at the window opening (Figure 4a) provided the components of inlet air velocity boundary condition for the CFD model (horizontal X component parallel to the window plane and vertical Y component). The horizontal Z component perpendicular to the external wall plane was not considered significant and was not measured, due to the relatively small size of the window awning gap and almost horizontal position of the boundary plane. Moreover, an air speed sensor [30] located at the window outlet (V1) (Figure 4b) provided the measurement of the speed of air exiting the room (vertical Y component), which was used for the validation purposes. Flags placed at both window openings (Figure 4a) provided an indication of the direction of the indoor flow (inlet – outlet).

The temperatures of internal walls were measured at one location for each wall by temperature sensors TMC6-HE [30] (Figure 4c). The floor temperature was measured at two locations inside the room by temperature sensors TMC20-HD [30] (Figure 4d). The surface temperatures of the column, external walls (below the windows) and the ceiling were measured using a thermal camera FLIR T335 [34].

Figure 3. The measurement setup.

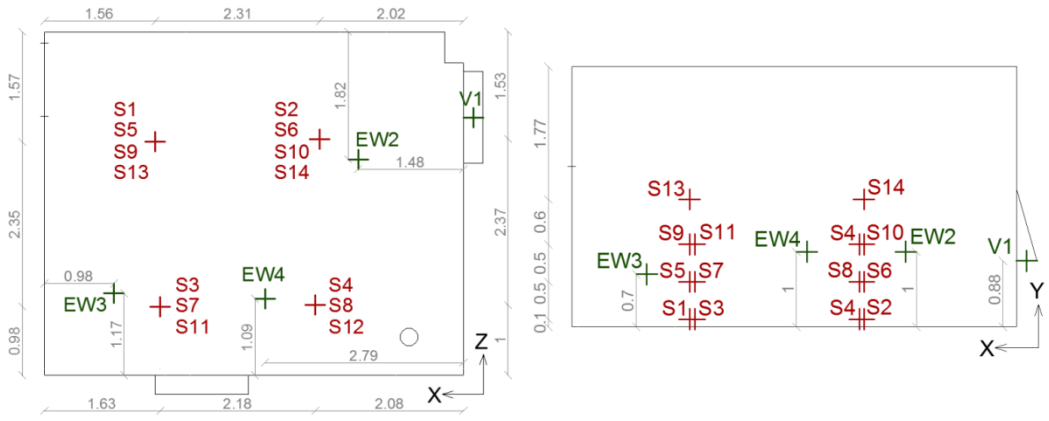

Please reference as:
Hajdukiewicz, M., Geron, M., & Keane, M.M., 2013. 'Calibrated CFD simulation to evaluate thermal comfort in a highly-glazed naturally ventilated room'. *Building and Environment*, 70, pp. 73-89. http://dx.doi.org/10.1016/j.buildenv.2013.08.020

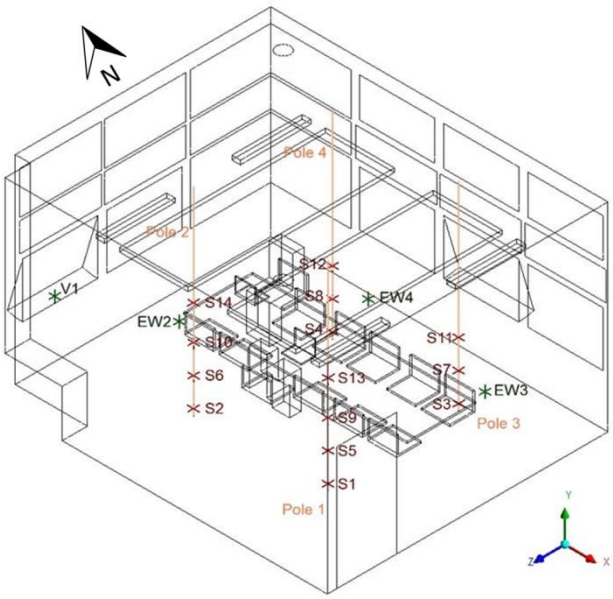

Figure 4. Air speed sensors at the window inlet (a) and window outlet (b); and temperature sensors at the wall (c) and floor (d).

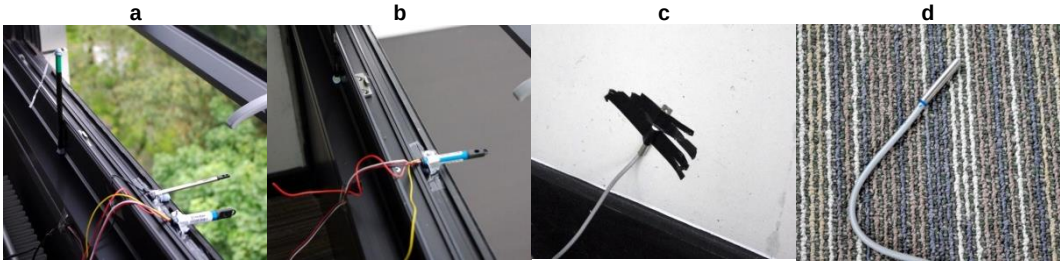

The Hobo U12 data loggers could measure air temperatures between -20 ^{o}C and 70 ^{o}C, with an accuracy of ± 0.35 ^{o}C (in a range between 0 - 50 ^{o}C). The Egg-Whisk sensors were capable of measuring indoor convection air speeds between 0.05 – 1 m/s with an accuracy of ± 0.01 m/s. The air speed sensors located at the window openings measured air speeds between 0.15 - 5 m/s, with accuracy greater of 10% of reading or ± 0.05 m/s, or 1% full-scale. The accuracy of the surface temperature sensors was ± 0.25 ^{o}C in a range between 0 - 50 ^{o}C. The measurement accuracy of the thermal camera was ± 2 ^{o}C or 2% of the reading.

The measurements of indoor air/surface temperatures and air speeds at window openings were taken with a time step of 1 minute; while, the indoor air speeds were measured by the Egg-Whisk sensors every second.

4.3. CFD analysis

The CFD simulation of the meeting room in the Engineering Building was performed using the commercial software Ansys CFX v.13.0 [35].The airflow and the air temperature stratification were simulated in a naturally ventilated room occupied by two people working on laptops. The settings of the CFD model imitated the conditions inside the room during the field measurements. The

Please reference as:
Hajdukiewicz, M., Geron, M., & Keane, M.M., 2013. 'Calibrated CFD simulation to evaluate thermal comfort in a highly-glazed naturally ventilated room'. *Building and Environment*, 70, pp. 73-89. http://dx.doi.org/10.1016/j.buildenv.2013.08.020

development of a validated CFD model of the meeting room followed the steps of the formal calibration methodology [23].

4.3.1. Geometry

The 3D geometry of the meeting room was created based on technical drawings, operation and maintenance (O&M) manuals and site visits. Since, a high level of detail in the CFD model would not influence the overall airflow inside the room but significantly increase grid and computational cost [35], the geometrical elements of the modelled meeting room, i.e. the occupants, windows, chairs and tables, were simplified in this work. Figure 5 shows the level of detail in the geometry of the modelled room.

Figure 5. The geometry of the meeting room CFD model.

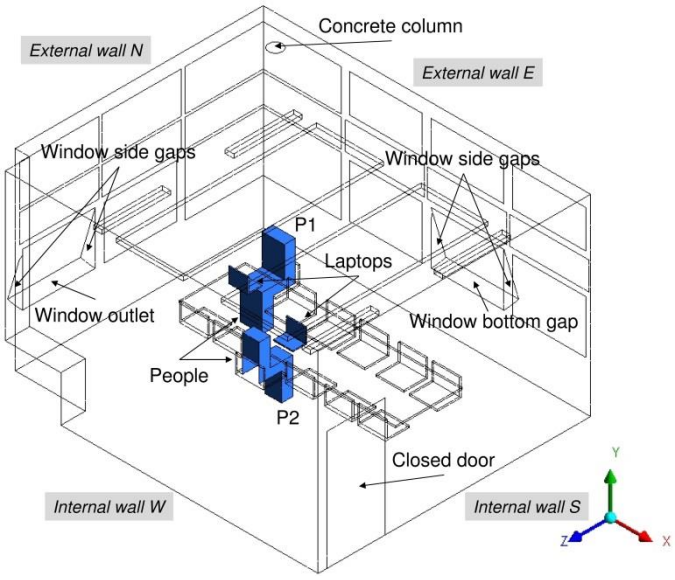

4.3.2. Boundary conditions

The boundary conditions for the CFD model, were provided by the automatic weather station installed at the NUI Galway campus [28], two air speed sensors placed at the centre of the window opening [30], surface temperature sensors [30], thermal camera images [34] and they were assumed from the typical values found in literature (e.g. human body heat flux, laptop heat flux, etc.).

The data supporting CFD simulations were gathered during the field measurements in the meeting room on August 17th, 2012. The external weather conditions, as well as indoor air speeds and air temperatures, were monitored throughout the day. The outdoor air entered the room through the east facing window (window bottom gap) and exited the room through the north facing window (window outlet). The modelled meeting room was occupied by two sitting people working on their laptops. The conditions over a 45 minute period in the afternoon, when outdoor and indoor conditions were relatively steady, were chosen to be used in the CFD simulation. The average values over the 45 minute period provided the boundary conditions and validation data for the model; while their variations were used in the parametric analysis. Table 1 presents the boundary conditions for the CFD model of the meeting room.

Please reference as:
Hajdukiewicz, M., Geron, M., & Keane, M.M., 2013. 'Calibrated CFD simulation to evaluate thermal comfort in a highly-glazed naturally ventilated room'. *Building and Environment*, 70, pp. 73-89. http://dx.doi.org/10.1016/j.buildenv.2013.08.020

Table 1. Boundary conditions for the CFD model of the meeting room.

Boundary	Type	Heat transfer	Mass & momentum	Radiation
Window bottom gap	Inlet	T_o = 20.82 [°C]	V_X = 0.47 [m/s] V_Y = 0.56 [m/s]	n/a
Window side gaps	Opening	T_o = 20.82 [°C]	$P_{relative}$ = 0 [Pa]	n/a
Window outlet	Opening	T_o = 20.82 [°C]	$P_{relative}$ = 0 [Pa]	n/a
Internal closed door	Wall	Adiabatic	No slip wall	ε = 0.9 DF = 1.0
External double glazed windows	Wall	h_c = 2.30 [W/m^{2}K] T_o = 20.82 [°C] $q_{radiative}$ = 203.10 [W/m^2]	No slip wall	ε = 0.9 DF = 1.0
Internal wall facing south	Wall	T_{wall} = 23.64 [°C]	No slip wall	ε = 0.9 DF = 1.0
Internal wall facing west	Wall	T_{wall} = 24.45 [°C]	No slip wall	ε = 0.9 DF = 1.0
External wall facing north	Wall	T_{wall} = 22.6 [°C]	No slip wall	ε = 0.9 DF = 1.0
External wall facing east	Wall	T_{wall} = 22.6 [°C]	No slip wall	ε = 0.9 DF = 1.0
Column	Wall	T_{wall} = 22.8 [°C]	No slip wall	ε = 0.9 DF = 1.0
Ceiling	Wall	T_{wall} = 23.0 [°C]	No slip wall	ε = 0.9 DF = 1.0
Floor	Wall	T_{wall} = 23.5 [°C]	No slip wall	ε = 0.9 DF = 1.0
People sitting	Wall	$q_{convective}$ = 18 [W/m^2] $q_{radiative}$ = 42 [W/m^2]	No slip wall	ε = 0.9 DF = 1.0
Laptops	Wall	$Q_{convective}$ = 131 [W]	No slip wall	ε = 0.9 DF = 1.0
Tables, chairs, sound panels and lamps	Wall	Adiabatic	No slip wall	ε = 0.9 DF = 1.0

T_o – outdoor temperature; T_{wall} – wall temperature; h_c – heat transfer coefficient; $q_{convective}$ – convective heat flux; $q_{radiative}$ – radiative heat flux; $Q_{convective}$ – convective heat source; V_x – air speed horizontal component parallel to the windows' plane; V_y – air speed vertical component; $P_{relative}$ – pressure relative to the reference pressure ($P_{reference}$ = 100200 Pa - absolute pressure datum from which all other pressure values were taken); ε – emissivity; DF – diffuse fraction;

The meeting room is a highly-glazed space, with windows covering the majority of external walls. Thus, the radiation model was included in the CFD simulation (simulation without radiation model activated, strongly underpredicted indoor air temperatures). A discrete transfer model (assumption of an isotropic scattering and reasonably homogenous system) was chosen in the analysis, since it is very efficient and provides accurate results [35]. For the period monitored the average global and diffuse solar irradiance were 445.63 W/m^2 and 203.10 W/m^2 respectively [28].The windows of the meeting room are facing north and east directions and the measurements, to support the CFD model, were taken in the afternoon. Thus, only the diffuse part of solar irradiance was considered in the CFD model. Moreover, the amount of solar irradiance transmitted through the window depends on the transmittance of the glass. In this case, the glass transmittance was not known. Thus, it was assumed that 100% of diffuse solar irradiance was transmitted inside the room. However, the variation of solar irradiance through the period monitored was included in the parametric analysis.

The diffuse solar irradiance was measured on a horizontal surface (received from the entire hemisphere, i.e. 180° field of view). The calculation of average (over period monitored) diffuse solar irradiance and approximate reflected solar irradiance (ground reflectivity was assumed 20% [25]) on a vertical window was not significantly different to the measured diffuse solar irradiance on a horizontal

Please reference as:
Hajdukiewicz, M., Geron, M., & Keane, M.M., 2013. 'Calibrated CFD simulation to evaluate thermal comfort in a highly-glazed naturally ventilated room'. *Building and Environment*, 70, pp. 73-89. http://dx.doi.org/10.1016/j.buildenv.2013.08.020

surface. Thus, in order to simplify the analysis, the average diffuse solar irradiance measured on a horizontal surface was used as a boundary condition for the vertical window.

The heat sources inside the room consisted of two people working on their laptops. The heat flux generated by people was taken as 60 W/m^2 for the seated person [25]. The convective and radiative heat fluxes from the people were set to 18 W/m^2 and 42 W/m^2 respectively (recommended convection to radiation ratio of 30:70 [36]). The laptops generated 131 W of electrical power each (it was assumed that all generated electrical power was transformed into heat). The surface temperatures of internal walls and the floor were specified in the model based on average measurements over the period monitored. The closed internal door, chairs, table, lamps and sound panels were assumed adiabatic. The emissivity and diffuse fraction (a ratio between the diffuse reflected energy and the total reflected energy at an opaque boundary) of all surfaces inside the room were assumed 0.9 and 1.0 respectively.

The outdoor air entered the room through the velocity inlet at the 27 cm wide bottom gap of the window awning. Two air velocity components were measured at the centre of the gap (X component – horizontal and parallel to the window plane, Y component - vertical) and the CFD boundary conditions were specified as the average measured values, constant over the whole velocity inlet. The air exited the room through the window outlet (27 cm wide gap), which was specified with no pressure difference between the boundary and outdoor conditions. Window side gaps (vertical triangular planes formed after opening the window) were modelled as openings at the same reference pressure as the outdoor conditions. The influence of the airflow through the window side gaps was not expected to be significant for the airflow inside the room.

4.3.3. Model setup

The steady state conditions were used in the CFD analysis of a single phase airflow inside the meeting room. The full buoyancy model, where the fluid density is evaluated utilising the ideal gas law, was applied. The air was modelled as an ideal gas with the reference buoyancy density of 1.173 kg/m^3.

The standard k-ε turbulence model was chosen for a good accuracy of the results with the robustness of the solution. Satisfactory convergence was achieved, using the criteria of 0.01% of root mean square residuals for mass and momentum equations, 1% of the energy conservation target and the numerical results at points of interest no longer changing with additional iterations. Simulations were performed with a single precision accuracy. The simulation with a double precision accuracy did not produce significantly different results from the results of a single precision accuracy; thus, the round-off error was not considered substantial in this case.

4.3.4. Model verification

The grid independence study of indoor air temperatures was performed in order to verify the CFD model solution. Three different meshes, successively refined (maximum element sizes for the coarse, medium and fine meshes were 0.21 m, 0.10 m and 0.07 m respectively), were created using unstructured elements (tetrahedrons, wedges, pyramids and hexahedrons) . The refinement ratio (r)

Please reference as:
Hajdukiewicz, M., Geron, M., & Keane, M.M., 2013. 'Calibrated CFD simulation to evaluate thermal comfort in a highly-glazed naturally ventilated room'. *Building and Environment*, 70, pp. 73-89. http://dx.doi.org/10.1016/j.buildenv.2013.08.020

for a 3D mesh is defined as the ratio between the number of grid elements in the fine (Δ_{fine}) and coarse (Δ_{coarse}) meshes:

$$r = \left(\frac{\Delta_{fine}}{\Delta_{coarse}} \right)^{\frac{1}{3}} \quad (1)$$

It is recommended that the grid refinement ratio must be greater than 1.3 [37] to allow the discretisation error to be separated from the other sources of error. The number of grid elements (Δ) and the refinement ratio (r) for each mesh are presented in Table 2.

Table 2. Grid parameters for three different mesh sizes.

Δ_3	Δ_2	Δ_1	r_{32}	r_{21}
479 289	1 066 002	2 480 318	1.31	1.33

Figure 6 demonstrates the qualitative grid verification. Vertical air temperature profiles along the room height are plotted for three mesh sizes (Δ3, Δ2 and Δ1). Presented profiles indicate a very close prediction between the medium (Δ2) and fine (Δ1) meshes (except the lower locations at the pole 3, where the prediction of Δ2 mesh is closer to Δ3 than Δ1). The discretisation error associated with the coarse mesh (Δ3) strongly affected the results, which failed to accurately predict air temperatures along poles 2, 3 and 4.

Figure 6. Simulated indoor air temperatures.

Please reference as:
Hajdukiewicz, M., Geron, M., & Keane, M.M., 2013. 'Calibrated CFD simulation to evaluate thermal comfort in a highly-glazed naturally ventilated room'. *Building and Environment*, 70, pp. 73-89. http://dx.doi.org/10.1016/j.buildenv.2013.08.020

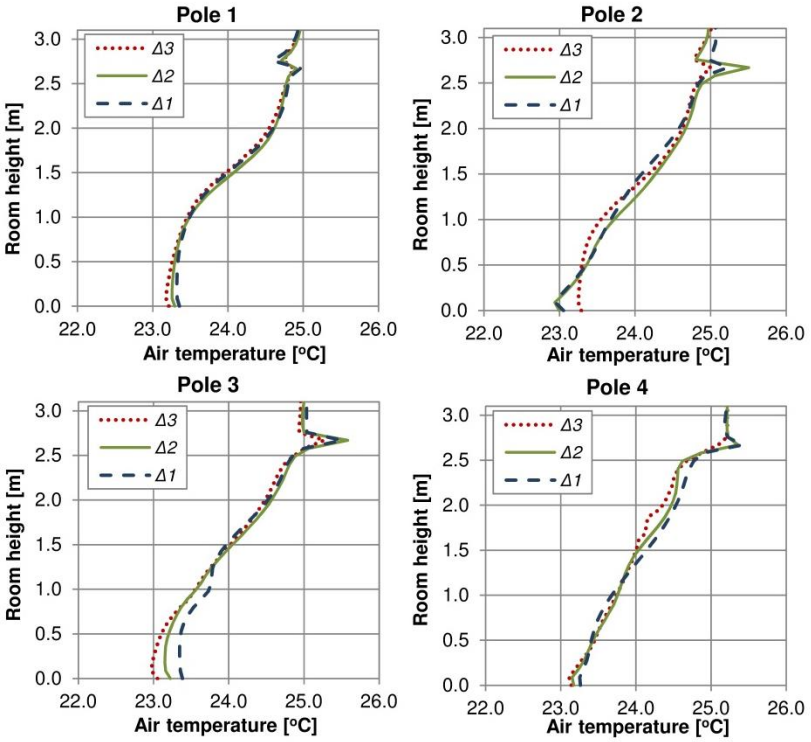

The quantitative grid verification can be performed using the grid convergence index (GCI) method [24]. Based on the Richardson extrapolation, the GCI for the fine grid solution helps to estimate the grid convergence error. The goal of the GCI method is to determine the error band for a given simulation result such that the exact solution is within that band with 95% confidence [38]. However, the ability to use the GCI method depends on the convergence conditions (such as monotonic or oscillatory convergence and divergence). For three successfully refined meshes, the convergence ratio (R) is calculated from [39]:

$$R = \frac{f_{medium} - f_{fine}}{f_{coarse} - f_{medium}} \tag{2}$$

where f_{fine}, f_{medium} and f_{coarse} are solutions of the fine, medium and coarse meshes respectively, and

$0 < R < 1 \rightarrow$ monotonic convergence

$-1 < R < 0 \rightarrow$ oscillatory convergence

$R > 1 \rightarrow$ monotonic divergence

$R < -1 \rightarrow$ oscillatory divergence

The *GCI* method can only be used for the monotonic convergence condition and, then, the grid convergence error is equal to the value of calculated *GCI* ($E = GCI^{fine}$). If the monotonic convergence is not observed the grid convergence error can be calculated from [38]:

$$E = 3\Delta_M = 3\max\left(\left| f_{coarse} - f_{fine} \right|\right) \tag{3}$$

The *GCI* is described as:

Please reference as:
Hajdukiewicz, M., Geron, M., & Keane, M.M., 2013. 'Calibrated CFD simulation to evaluate thermal comfort in a highly-glazed naturally ventilated room'. *Building and Environment*, 70, pp. 73-89. http://dx.doi.org/10.1016/j.buildenv.2013.08.020

$$GCI^{fine} = F_S \frac{\varepsilon}{r^p - 1} \quad (4)$$

where F_s is the safety factor, ε is a relative error between the coarse and fine grid solutions and p is the order of convergence.

In this work, the quantitative grid verification could have been performed using the *GCI* method (Equation 4) only for two sensor locations where a monotonic convergence was observed (S1 and S6). At four locations where an oscillatory convergence was observed, the grid convergence error was estimated using Equation 3. For the remaining eight locations with a clearly divergent solution (S3-S5, S7, S8, S11, S12 and S14) no grid verification error could have been calculated and only qualitative grid verification was carried out. The calculated values of grid convergence error for the simulated air temperatures at six locations (S1, S2, S6, S9, S10 and S13) were compared to the measurement accuracy at the same locations. This was done in order to justify the choice of the grid independent solution at the reasonable computational cost (Table 3).

Table 3. Grid convergence error and measurement accuracy for indoor air temperatures.

Sensor location	R [-]	Convergence type	E_{32} [%]	E_{21} [%]	Measurement accuracy [%]
S1	0.82	Monotonic conv.	2.04	1.62	1.49
S2	-0.01	Oscillatory conv.	3.88	0.04	1.49
S3	1.06	Monotonic diverg.	n/a	n/a	1.50
S4	2.46	Monotonic diverg.	n/a	n/a	1.50
S5	1.57	Monotonic diverg.	n/a	n/a	1.47
S6	0.09	Monotonic conv.	0.05	0.00	1.48
S7	1.77	Monotonic diverg.	n/a	n/a	1.48
S8	12.79	Monotonic diverg.	n/a	n/a	1.49
S9	-0.42	Oscillatory conv.	0.61	0.26	1.46
S10	-0.47	Oscillatory conv.	2.31	1.08	1.46
S11	5.60	Monotonic diverg.	n/a	n/a	1.47
S12	9.38	Monotonic diverg.	n/a	n/a	1.48
S13	-0.66	Oscillatory conv.	1.32	0.86	1.45
S14	-3.58	Monotonic diverg.	n/a	n/a	1.46

Despite some problems of convergence at some points of interest, the medium mesh size Δ_2 was chosen for further analysis. The air temperature profiles inside the room (Figure 6) showed that the results of the medium (Δ_2) and fine (Δ_1) meshes were very close. Moreover, low values of the grid convergence error E_{21} in comparison with the measurement accuracy proved a good accuracy of the Δ_2 mesh results, at a reasonable computational cost. Table 4 shows the properties of the Δ_2 mesh, which indicate a good mesh quality.

Table 4. Properties of the Δ_2 mesh (average over the domain).

Element quality	0.73 [-]

Please reference as:
Hajdukiewicz, M., Geron, M., & Keane, M.M., 2013. 'Calibrated CFD simulation to evaluate thermal comfort in a highly-glazed naturally ventilated room'. *Building and Environment*, 70, pp. 73-89. http://dx.doi.org/10.1016/j.buildenv.2013.08.020

Aspect ratio	2.68 [-]
Skewness	0.24 [-]
Maximum corner angle	90.25 [deg]

4.3.5. Model results

Table 5 lists the properties of the simulated flow inside the room. The Reynolds number confirmed the flow was of turbulent nature. With the expected range of indoor air temperatures the dynamic viscosity and thermal conductivity were assumed constant.

Table 5. Properties of the flow inside the modelled room.

Reynolds number (considering the length of inlet window gap)	12 119 [-]
Prandtl number	0.70462 [-]
Dynamic viscosity	$1.831e^{-5}$ [kg/(ms)]
Thermal conductivity	$2.61e^{-2}$ [W/(mK)]

Figure 7 demonstrates the air temperature stratification and airflow distribution inside the modelled room. The location of three vertical planes: A and C (through the occupants), B (through the middle of the window inlet) are used to show the CFD results.

The results showed the airflow inside the room was strongly wind-driven. The cold air entered the room through the window inlet (plane B in Figure 7) and exited through the window outlet. Figure 8a shows that the airflow streamlines were spread inside the whole room. The heat plumes above the sitting people (planes A and C in Figure 7) were relatively small.

The average air speeds inside the room ranged from 0.14 m/s at the ankles level (h = 0.1 m); 0.08 m/s at the sitting person's waist level (h = 0.6 m); 0.10 m/s at the sitting person's head or standing person's waist level (h = 1.1 m); and 0.08 m/s at the standing person's head level (h = 1.7 m). Respectively, the average air temperatures were 23.11 ^{o}C at the ankles level; 23.41 ^{o}C at the sitting person's waist level; 23.61 ^{o}C at the sitting person's head or standing person's waist level; and 24.16 ^{o}C at the standing person's head level. The average vertical air temperature difference between the head (h = 1.1 m) and ankles (h = 0.1 m) level was less than 2 ^{o}C. This caused a dissatisfaction level of only 6% [40].

Previous research found that the level of occupant thermal acceptability at preferred temperatures was unaffected by air speeds of 0.25 m/s or lower [41]. Figure 8b presents an isosurface of indoor air speeds of 0.25 m/s (higher air speeds were present inside this isosurface). It is clear that the airflow jet generated at the window inlet entered the room almost vertically, dropped down near the corner of the room and aimed towards the window outlet at the floor level. This airflow jet omitted the occupants, except the ankles level of the person P1 situated in the room corner (which might have caused a local discomfort of this person). Moreover, there were two small airflow jets of 0.25 m/s air speed generated above the laptops with convective heat fluxes. There were no 0.25 m/s air speed

Please reference as:
Hajdukiewicz, M., Geron, M., & Keane, M.M., 2013. 'Calibrated CFD simulation to evaluate thermal comfort in a highly-glazed naturally ventilated room'. *Building and Environment*, 70, pp. 73-89. http://dx.doi.org/10.1016/j.buildenv.2013.08.020

jets created above the occupants. This was due to the fact that the heat generated by the occupants was transferred mostly through radiation, as opposed to convection.

Figure 7. Verified model results.

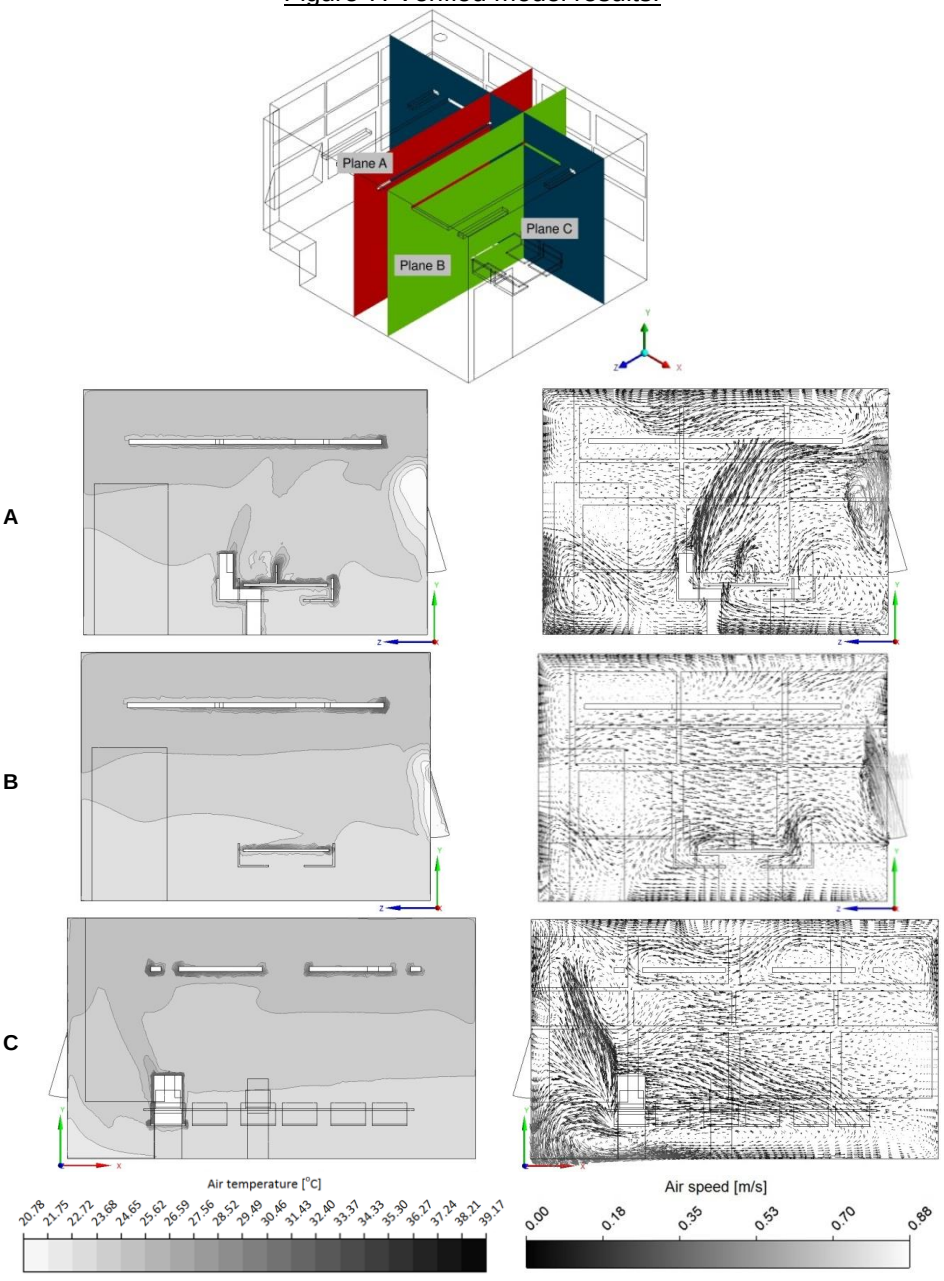

Figure 8. Indoor airflow streamlines from the window inlet towards the window outlet (a) and indoor air speeds of 0.25 m/s (b).

Please reference as:
Hajdukiewicz, M., Geron, M., & Keane, M.M., 2013. 'Calibrated CFD simulation to evaluate thermal comfort in a highly-glazed naturally ventilated room'. *Building and Environment*, 70, pp. 73-89. http://dx.doi.org/10.1016/j.buildenv.2013.08.020

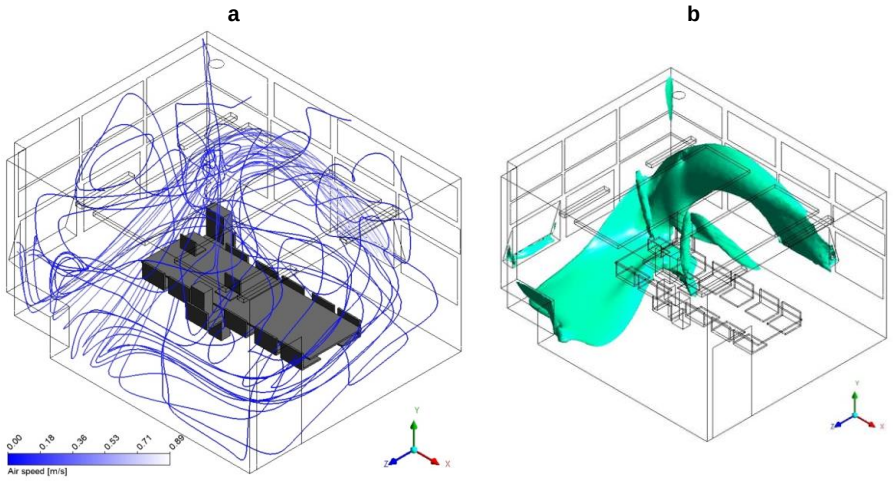

4.4. Model validation

The first step of the validation procedure consisted of a qualitative comparison between the measured and simulated data (Figure 9 and Figure 10).

Figure 9. Qualitative comparison of measured and simulated indoor air speeds (range of measured data shown).

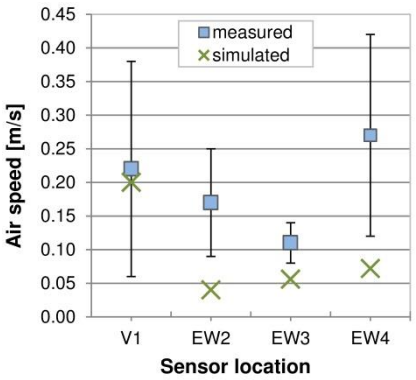

Figure 10. Qualitative comparison of measured and simulated indoor air temperatures (range of measured data shown).

Please reference as:
Hajdukiewicz, M., Geron, M., & Keane, M.M., 2013. 'Calibrated CFD simulation to evaluate thermal comfort in a highly-glazed naturally ventilated room'. *Building and Environment*, 70, pp. 73-89. http://dx.doi.org/10.1016/j.buildenv.2013.08.020

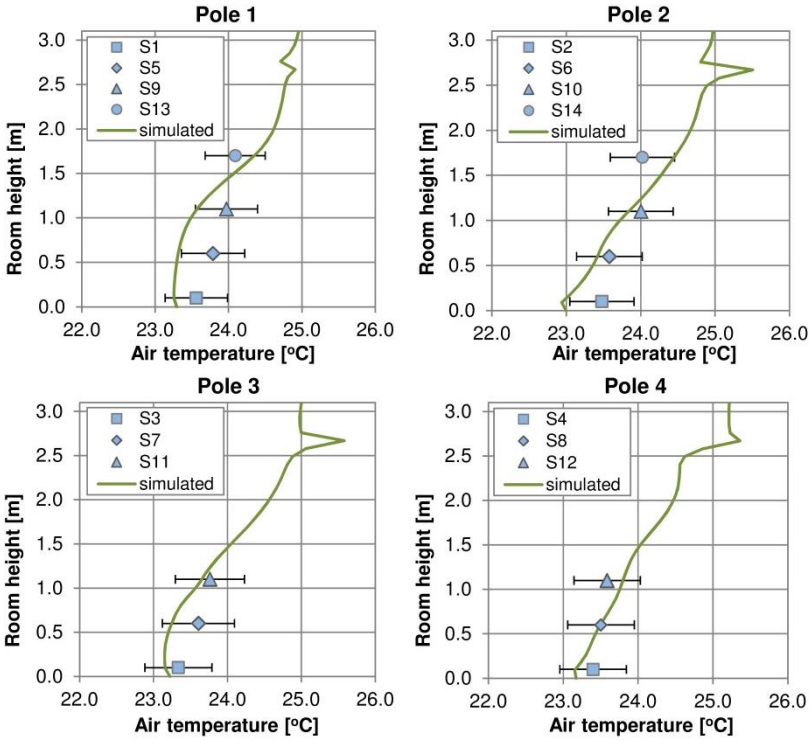

The validation criteria for this work were defined as 0.15 m/s absolute difference between measured and simulated air speeds, and 0.50 °C absolute difference between measured and simulated air temperatures. The validation criteria were based on the maximum uncertainties in measured data (0.15 m/s for air speeds and 0.49 °C for air temperatures). The uncertainties included the measurement uncertainty (standard deviation) and sensors accuracy (± 0.01 m/s for air speeds and ± 0.35 °C for air temperatures).

Table 6 shows the absolute differences between measured and simulated indoor air speeds and air temperatures. The model met the validation criterion when predicting air temperatures (except the location S2, where the air temperature was slightly under predicted). At the EW4 Egg-Whisk location, which was the closest to the window inlet, the model failed to predict the air speed accurately. However, despite the excess over the validation criterion, the difference between the measured and simulated value at the location EW4 was not extremely high; and may be considered acceptable.

Table 6. Quantitative comparison of measured and simulated indoor data (values in bold red exceed validation criteria).

Data type	Location	Measured	Simulated	Absolute difference
Air speed [m/s]	V1	0.22	0.20	0.02
	EW2	0.17	0.04	0.13
	EW3	0.11	0.06	0.05
	EW4	0.27	0.07	**0.20**
Air temperature [°C]	S1	23.56	23.26	0.30
	S2	23.48	22.95	**0.53**
	S3	23.34	23.16	0.18
	S4	23.40	23.16	0.24

Please reference as:
Hajdukiewicz, M., Geron, M., & Keane, M.M., 2013. 'Calibrated CFD simulation to evaluate thermal comfort in a highly-glazed naturally ventilated room'. *Building and Environment*, 70, pp. 73-89. http://dx.doi.org/10.1016/j.buildenv.2013.08.020

	S5	23.79	23.31	0.47
	S6	23.58	23.42	0.16
	S7	23.61	23.25	0.36
	S8	23.50	23.49	0.01
	S9	23.97	23.57	0.40
	S10	24.00	23.84	0.16
	S11	23.76	23.65	0.11
	S12	23.59	23.80	0.21
	S13	24.09	24.35	0.26
	S14	24.02	24.24	0.42

Table 7 presents a quantitative comparison between measured and simulated turbulence intensities (*TI*). The turbulence intensity is defined as:

$$TI = \frac{u'}{U} \tag{5}$$

where *u'* is the root mean square or standard deviation of the turbulent velocity fluctuations at a particular location over the specified period of time; and *U* is an average air velocity at the same location over the same period of time.

In the environments equipped with the mixed-flow air distribution the turbulence intensity may vary between 30% – 60% [40]. In this study, measured turbulence intensities at four locations were lower than 60%. At the location EW3 the turbulence intensity was lower than 30%; however, it is acceptable in the environments without mechanical ventilation [40]. Furthermore, it can be seen that the turbulence intensity was strongly overestimated at the location EW2 (the closest to the window outlet) and underestimated at the location EW4 (the closest to the window inlet). At the V1 and EW3 locations the simulated turbulence intensity was predicted quite well (error of less than 34%). The EW3 sensor was located in the southeast corner of the room, free of the main wind-driven flow and, thus, the simulated turbulence intensity was more accurate there. The measurement at the V1 location (window outlet) strongly depended on the air velocity at the inlet. For this reason the airflow was well established there and easier to predict than at the locations inside the room.

Table 7. Turbulence intensities at the indoor air speed measurement locations.

Location	$TI_{measured}$ [%]	$TI_{simulated}$ [%]	*Error* [%]
V1	50.8	33.6	33.8
EW2	41.0	75.9	85.0
EW3	22.6	29.9	32.2
EW4	53.0	20.3	61.7

4.5. Parametric analysis

The first step of the parametric analysis consisted of assessing the plausible ranges of numerical input parameters (Table 8). The selection of input parameters was influenced by the results of the previous study published by the authors [23]. The air reference density (*RefDen*), inlet air velocity components (*AirVelX* and *AirVelY*) and the inlet air temperature (*AirTemp*) were expected to have a strong impact on the environment in the meeting room. The solar radiation (*WinRad*) was included

Please reference as:
Hajdukiewicz, M., Geron, M., & Keane, M.M., 2013. 'Calibrated CFD simulation to evaluate thermal comfort in a highly-glazed naturally ventilated room'. *Building and Environment*, 70, pp. 73-89. http://dx.doi.org/10.1016/j.buildenv.2013.08.020

because the room is highly-glazed. The heat fluxes from the occupants (*PerHeat* and *PerRad*) and laptops (*CompHeat*) were also expected to be influential.

Table 8. Input parameters and their ranges.

Input parameter	Description	Lower bound	Upper bound
RefDen	Air density	1.163 [kg/m^3]	1.183 [kg/m^3]
AirTemp	Outdoor air temperature	20.63 [^{o}C]	21.02 [^{o}C]
AirVelX	Inlet air velocity (horizontal component, parallel to the window plane)	0.30 [m/s]	0.64 [m/s]
AirVelY	Inlet air velocity (vertical component)	0.38 [m/s]	0.73 [m/s]
CompHeat	Laptops convective heat source	105 [W]	157 [W]
PerHeat	People convective heat flux	14.4 [W/m^2]	21.6 [W/m^2]
PerRad	People radiative heat flux	33.6 [W/m^2]	50.4 [W/m^2]
WinRad	Solar radiation at windows	135.74 [W/m^2]	270.46 [W/m^2]

The input parameter ranges were related to the variation in the measurements and uncertainty in assumptions of the boundary conditions. The range of the air reference density (*RefDen*) was calculated using the ideal gas law equation based on the minimum and maximum expected indoor air temperatures. The ranges of the inlet air temperature (*AirTemp*), inlet air velocity components (*AirVelX* and *AirVelY*) and solar radiation (*WinRad*) were based on the average measurements ± standard deviation in air temperature, diffuse solar irradiance (weather station) and air speeds (window inlet). The heat flux generated by people was taken as 60 W/m^2 for the seated person [25]. It was assumed the heat from the people was transferred through convection (*PerHeat*) and radiation (*PerRad*) with a C:R ratio of 30:70 [36]. The ranges of the convective and radiative heat fluxes were specified as the average values ± 20%. The range of the heat generated by the laptops (*CompHeat*) was based on the manufacturer's specification ± 20%.

In the next step of the parametric analysis, the design of experiments method (DOE) (sampling method) aimed to locate the sample points in a way that random input parameters were explored in the most efficient way (i.e. the required information was obtained with minimum sampling points). Sample points located efficiently reduced the computational time and increased the accuracy of the response surface derived from the results of the simulations with sampling points as input parameters. In this research, the determination of the sample points for the input parameters was performed using the central composite design method with fractional factorial design. Central composite design provides traditional DOE sampling and combines one centre point, points along the axis of the input parameters and the points determined by a fractional factorial design. Factorial design allows for changing all input parameters within the specified ranges at the same time, instead of one parameter at the time. The fractional design is typically used for a larger number of input parameters (as opposed to a full design, which is used for five or less input parameters), since it reduces the computational cost by estimating only a few combinations between variables.

Please reference as:
Hajdukiewicz, M., Geron, M., & Keane, M.M., 2013. 'Calibrated CFD simulation to evaluate thermal comfort in a highly-glazed naturally ventilated room'. *Building and Environment*, 70, pp. 73-89. http://dx.doi.org/10.1016/j.buildenv.2013.08.020

In this work, for the selected eight input parameters, central composite design method generated 81 design points (sets of varying input parameters), which provided boundary conditions for 81 CFD models to be solved. For one of the design points, specifying the input inlet vertical velocity as the minimum value from the specified parameter range and keeping other parameters at their base values simulated a maximum change (from the base model result) of 0.11 m/s in the output indoor air speed at the location V1. For another design point, changing all of the input parameters within their ranges caused a maximum change in indoor air temperature of 0.72 ^{o}C at location S13. Based on the 81 sets of input boundary conditions, together with the relevant output indoor air speeds and air temperatures, the response surfaces were created using regression analysis with a second order approximation [42].

The accuracy of the fit of the predicted response values in the response surfaces generated by 81 CFD models was estimated using the coefficient of determination R^2 (Table 9). The R^2 values for indoor air speeds and air temperatures simulated in this work indicated a good accuracy of the responses' prediction.

Table 9. Coefficient of determination for simulated indoor air speeds and air temperatures.

Measurement	Sensor location	R^2
Air speed [m/s]	V1	0.994
	EW2	0.932
	EW3	0.857
	EW4	0.815
Air temperature [^{o}C]	S1	0.977
	S2	0.989
	S3	0.970
	S4	0.936
	S5	0.988
	S6	0.979
	S7	0.986
	S8	0.987
	S9	0.997
	S10	0.995
	S11	0.995
	S12	0.992
	S13	0.998
	S14	0.997

Figure 11 graphs the global sensitivities of the output air speeds and air temperatures inside the room to input boundary conditions. The global sensitivities were calculated based on the coefficient in the second order response surface regression model, which was the measurement of the expected change in the output parameters with varying inputs. The vertical component of inlet air velocity (*AirVelY*) influenced air speeds inside the room the most. Generally, higher the inlet air velocity vertical component, higher were the indoor air speeds (except at the location EW3, where the measured air speed was inversely proportional to the inlet air velocity vertical component). The indoor air temperatures were mostly influenced by the inlet velocity vertical component (*AirVelY*) (inversely

Please reference as:
Hajdukiewicz, M., Geron, M., & Keane, M.M., 2013. 'Calibrated CFD simulation to evaluate thermal comfort in a highly-glazed naturally ventilated room'. *Building and Environment*, 70, pp. 73-89. http://dx.doi.org/10.1016/j.buildenv.2013.08.020

proportional), solar radiation through the windows (*WinRad*), inlet velocity horizontal component (*AirVelX*) and outdoor air temperature (*AirTemp*) (all proportional). Moreover, changing the input parameters had the strongest impact on air speed changes at the location V1 (0.15 m/s) and the lowest at the location EW2 (0.05 m/s). The indoor air temperatures were the most sensitive (to changing input boundary conditions) at locations S13 (1.33 °C) and S14 (1.18 °C); and the least sensitive at locations S1 (0.47 °C), S3 (0.54 °C) and S4 (0.51 °C).

Figure 11. Sensitivity of indoor air speeds and air temperatures to input boundary conditions.

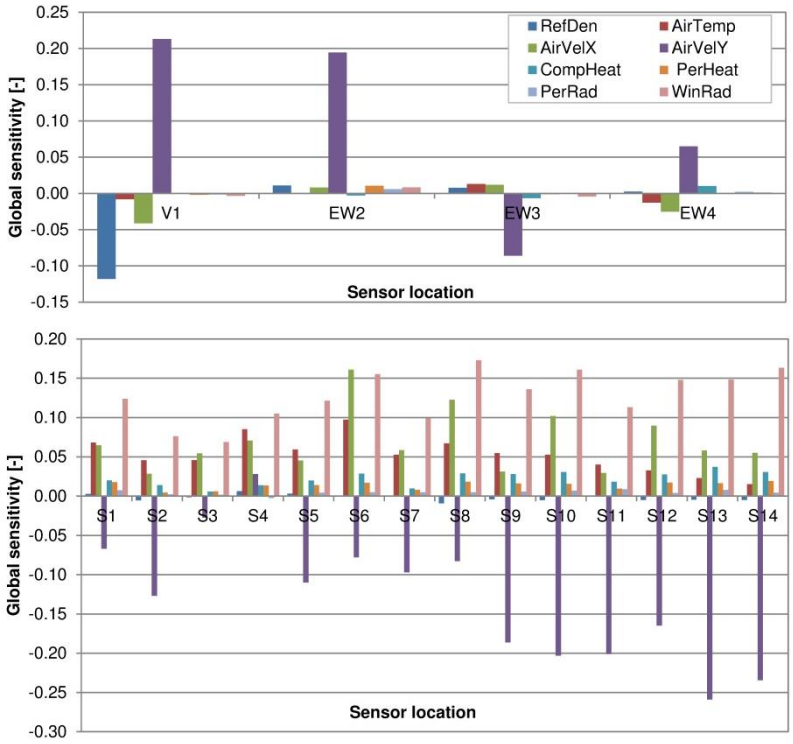

Figure 12 displays the impact of two inlet velocity components (*AirVelX* and *AirVelY*) on indoor air speeds. The parametric study showed that, by changing input parameters within the possible ranges, it was achievable to meet the validation criterion at location EW4 (the closest to the window inlet). However, this would influence the results at other indoor locations, which would then not comply with the validation criteria. Moreover, the underprediction of the EW4 air speed by the model might have been caused by the simplification of the inlet boundary condition and the assumption of the uniform conditions along the window gap. Figure 13 demonstrates the impact of the inlet velocity vertical components (*AirVelY*) and solar irradiance through the windows (*WinRad*) on indoor air temperatures at the locations with the highest absolute difference between measured and simulated data. Similar patterns regarding the responses to changing input air velocity vertical component and solar irradiance are observed at those locations (S2, S5, S9 and S14).

Figure 12. Indoor air speed responses to changing input air velocity components.

V1 **EW2**

Please reference as:
Hajdukiewicz, M., Geron, M., & Keane, M.M., 2013. 'Calibrated CFD simulation to evaluate thermal comfort in a highly-glazed naturally ventilated room'. *Building and Environment*, 70, pp. 73-89. http://dx.doi.org/10.1016/j.buildenv.2013.08.020

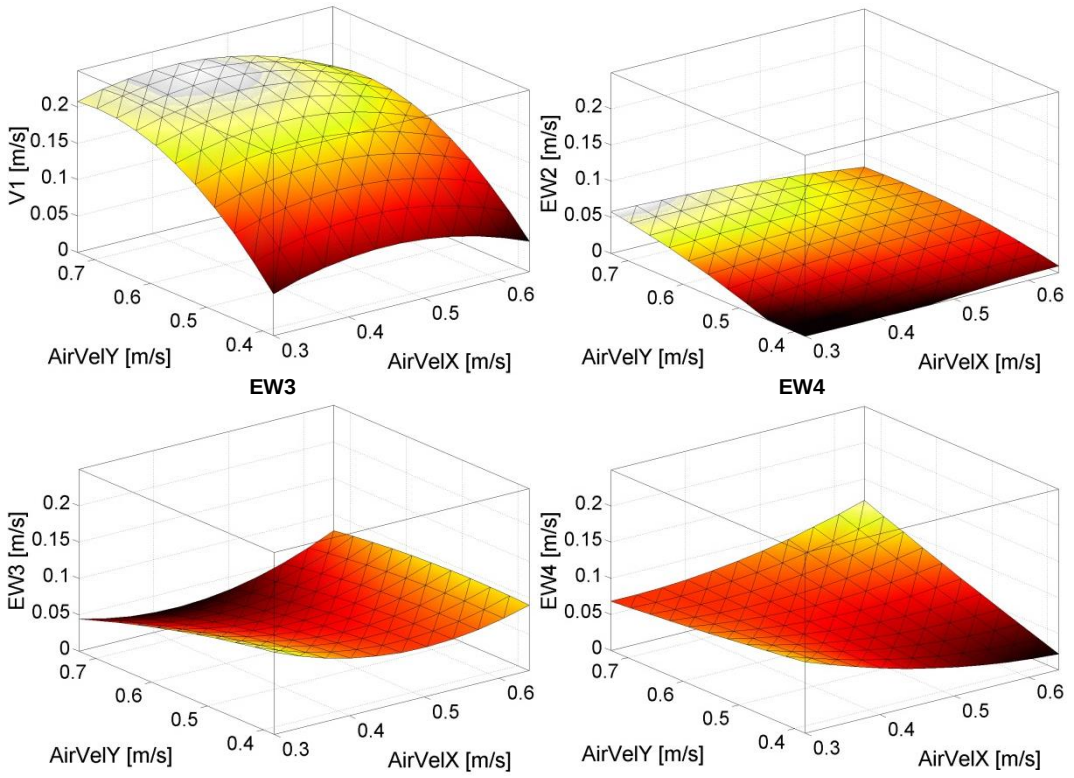

Figure 13. Indoor air temperature responses to changing input air velocity vertical component and solar irradiance.

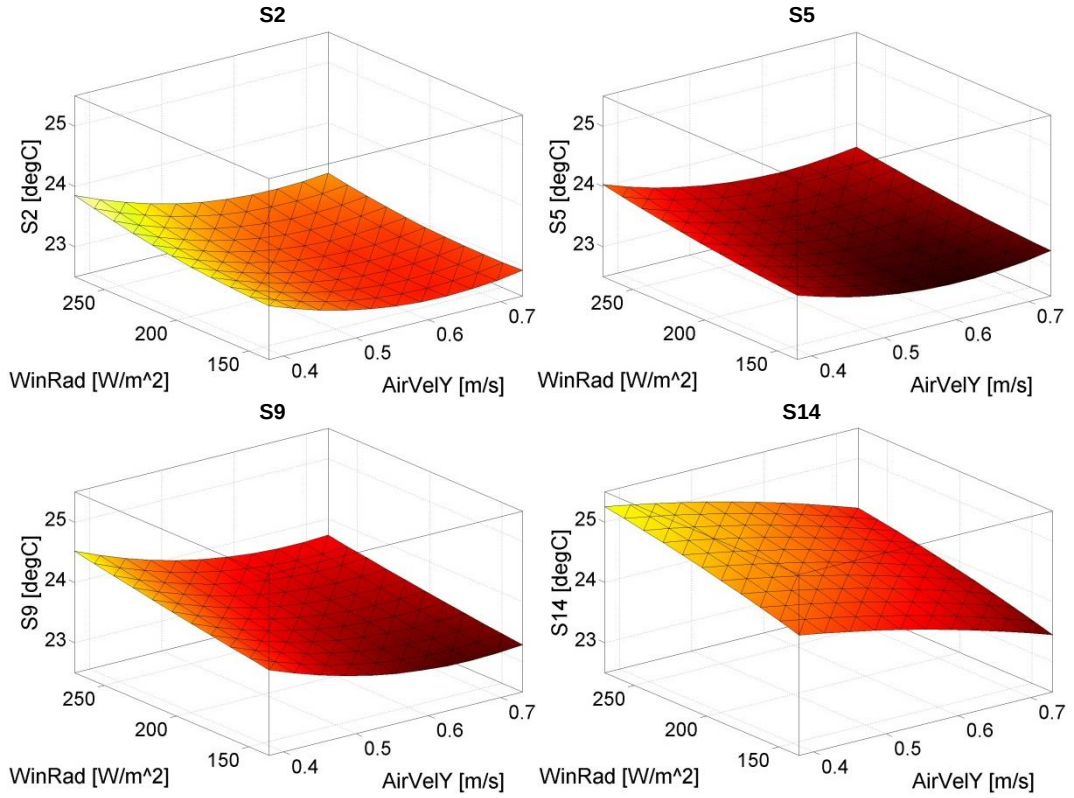

Please reference as:
Hajdukiewicz, M., Geron, M., & Keane, M.M., 2013. 'Calibrated CFD simulation to evaluate thermal comfort in a highly-glazed naturally ventilated room'. *Building and Environment*, 70, pp. 73-89. http://dx.doi.org/10.1016/j.buildenv.2013.08.020

4.6. Thermal comfort

Thermal comfort expresses occupants' satisfaction with thermal environment in buildings. Thermal comfort is determined using the predicted mean vote (*PMV*), predicted percentage of dissatisfied (*PPD*) and local thermal comfort criteria [40].

This work utilised field measurements and validated CFD model in order to determine global and local thermal comfort indices and ensure acceptable environmental conditions in the Engineering Building meeting room.

4.6.1. *PMV & PPD*

The *PMV* and *PPD* indicate warm and cold discomfort for the whole body of the occupant. The *PMV* predicts the mean value of the thermal votes of a large group of occupants exposed to the same environment, and is expressed by the thermal sensation scale (+3 hot, +2 warm, +1 slightly warm, 0 neutral, -1 slightly cool, -2 cool, -3 cold) [40]. The *PPD* quantitatively predicts the percentage of thermally dissatisfied occupants (those, who would vote hot, warm, cold or cool in the thermal sensation scale) [40]. The *PMV* value can be calculated based on Equations 6 - 9 [40]:

$$PMV = \left[0.303 * e^{-0.036M} + 0.028\right] * \begin{Bmatrix} (M-W) - 3.05*10^{-3} * \left[5733 - 6.99*(M-W) - p_a\right] - 0.42*\left[(M-W) - 58.15\right] \\ -1.7*10^{-5} * M * (5867 - p_a) - 0.0014 * M * (34 - t_a) \\ -3.96*10^{-8} * f_{cl} * \left[(t_{cl}+273)^4 - (t_r+273)^4\right] - f_{cl} * h_c * (t_{cl} - t_a) \end{Bmatrix} \quad (6)$$

$$t_{cl} = 35.7 - 0.028*(M-W) - I_{cl} * \left\{3.96*10^{-8} * f_{cl} * \left[(t_{cl}+273)^4 - (t_r+273)^4\right] + f_{cl} * h_c * (t_{cl} - t_a)\right\} \quad (7)$$

$$h_c = \begin{Bmatrix} 2.38*\left|t_{cl} - t_a\right|^{0.25} \; for 2.38*\left|t_{cl} - t_a\right|^{0.25} \rangle 12.1*\sqrt{v_{ar}} \\ 12.1*\sqrt{v_{ar}} \; for 2.38*\left|t_{cl} - t_a\right|^{0.25} \langle 12.1*\sqrt{v_{ar}} \end{Bmatrix} \quad (8)$$

$$f_{cl} = \begin{Bmatrix} 1.00 + 1.290 * I_{cl} \; for I_{cl} \le 0.078 m^2 K/W \\ 1.05 + 0.645 * I_{cl} \; for I_{cl} \rangle 0.078 m^2 K/W \end{Bmatrix} \quad (9)$$

Where, M – metabolic rate [W/m^2]; W – effective mechanical power [W/m^2]; I_{cl} – clothing insulation [m^{2}K/W]; f_{cl} – clothing surface area factor [-]; t_a – air temperature [^{o}C]; t_r – mean radiant temperature [^{o}C]; v_{ar} – relative air velocity [m/s]; p_a – water vapour partial pressure [Pa]; h_c – convective heat transfer coefficient at the body surface [W/(m^{2}K)]; t_{cl} – clothing surface temperature [^{o}C].

Metabolic rate for the occupants and clothing insulation were assumed as standard values [25], [40]; relative humidity was the average relative humidity measured in the room at locations (S1 – S14); air temperature, relative air velocity and mean radiant temperature were the average values of air temperature, relative air velocity and mean radiant temperature inside the room simulated by the calibrated CFD model.

Please reference as:
Hajdukiewicz, M., Geron, M., & Keane, M.M., 2013. 'Calibrated CFD simulation to evaluate thermal comfort in a highly-glazed naturally ventilated room'. *Building and Environment*, 70, pp. 73-89. http://dx.doi.org/10.1016/j.buildenv.2013.08.020

The *PPD* is calculated from Equation 10 [40] using the *PMV* value.

$$PPD = 100 - 95 * e^{-0.03353*PMV^4 - 0.2179*PMV^2} \quad (10)$$

Table 10 shows the *PMV* and *PPD* values for the occupants of the meeting room in the Engineering Building. Those values indicate an almost neutral thermal sensation with only 5% of thermally dissatisfied people.

Table 10. *PMV* and *PPD* for the occupants of the meeting room.

PMV [-]	- 0.1
PPD [%]	5.2

4.6.2. Local thermal comfort

Thermal dissatisfaction of building occupants can be caused by unwanted cooling or heating of a particular part of their body, called local discomfort. The most common source of local discomfort in buildings is draught. Occupants comfort is also influenced by a vertical air temperature difference (between head and ankles), floor temperature or radiant asymmetry [40]. Table 11 lists local thermal discomfort indices for two occupants (P1 and P2 shown in Figure 5) of the meeting room.

Table 11. Local thermal discomfort indices for two occupants of the meeting room.

Criteria	Person P1	Person P2
DR [%]	5.3	7.1
$PD_{\text{vertical temperature difference}}$ [%]	1.7	0.8
$PD_{\text{floor temperature}}$ [%]	5.5	

4.6.2.1. Draught rate

The draught rate (*DR*) higher than 15% is considered unacceptable [43]. Thus, the calculated *DR* in the meeting room (5.3% for P1 and 7.1% for P2) did not cause local discomfort of the room occupants. The *DR* was calculated based on Ref. [40] using simulated (CFD model) local air temperature, local mean air velocity and local turbulence intensity at neck level (*h* = 1.0 m) for each occupant.

4.6.2.2. Vertical air temperature difference

The difference in air temperature between the head and ankles level may cause local discomfort for the occupants. Typically, the air temperature increases upwards (as in the case of the meeting room). However, when the thermal stratification is in the opposite direction, it is more favourable for the occupants. The vertical air temperature difference for occupants P1 (2.01 ^{o}C) and P2 (1.10 ^{o}C) in the meeting room indicated the thermal dissatisfaction level lower than 2%. The percentage of dissatisfied due to vertical air temperature difference ($PD_{vertical\ temperature\ difference}$) was calculated based on Ref. [40] using the simulated (CFD model) vertical air temperature difference between head (*h* = 1.1 m) and ankles (*h* = 0.1 m) of the occupants (both were averaged over eight points around occupants' head and ankles).

4.6.2.3. Warm and cold floor

Please reference as:
Hajdukiewicz, M., Geron, M., & Keane, M.M., 2013. 'Calibrated CFD simulation to evaluate thermal comfort in a highly-glazed naturally ventilated room'. *Building and Environment*, 70, pp. 73-89. http://dx.doi.org/10.1016/j.buildenv.2013.08.020

The floor temperature, rather than the floor covering material, is the most important factor for indoor thermal comfort of people wearing shoes. Thus, building occupants may feel uncomfortable due to too warm or too cold floor surface. The limit for floor temperature was specified as 19 – 29 °C [44]. In the case of the meeting room, the floor temperature of 23.50 °C caused a dissatisfaction level of just above 5%. The percentage of dissatisfied due to floor temperature ($PD_{floor\ temperature}$) was calculated based on Ref. [40] using measured (average over two locations) floor temperature.

4.6.2.4. Radiant asymmetry

Radiant temperature asymmetry may also cause local discomfort for building occupants, due to cold windows, uninsulated walls, improperly sized heating panels, etc. [25]. The percentage of dissatisfied due to radiant asymmetry (by warm/cool ceiling or warm/cool wall) can be calculated based on Ref. [40]. However, in this case, the occupants were not affected by any hot and cold surfaces (t_{floor} = 23.50 °C, $t_{ceiling}$= 23.00 °C, $t_{wall\ S}$ = 23.64 °C, $t_{wall\ N}$ = 22.60 °C, $t_{wall\ E}$ = 22.60 °C, $t_{wall\ W}$ = 24.45 °C, $t_{ave.windows}$ = 24.42 °C, remaining surfaces were adiabatic and there were no other heat sources than occupants and laptops) or direct sunlight (only diffuse solar irradiance through windows was present). Thus, radiant asymmetry was not considered in this case.

4.6.3. Operative temperature

The operative temperature is a uniform temperature of an imaginary black enclosure, where an occupant would exchange the same amount of heat through radiation and convection as in the actual non-uniform environment [40]. The operative temperature combines the air temperature and mean radiant temperature to express their joint effect on thermal comfort of building occupants. Table 12 shows the average, minimum and maximum simulated operative temperature inside the meeting room. The operative temperature was simulated by the CFD model according to Ref. [45].

Table 12. Simulated operative temperatures inside the meeting room.

AVE t_c [°C]	25.35
MIN t_c [°C]	22.12
MAX t_c [°C]	36.25

For the clothing insulation of 0.7 clo and metabolic rate of 60 W/m^2 the optimum operative temperature should be about 26 °C [40]. This shows that the average simulated operative temperature in the meeting room (25.35 °C) was very close to the optimum value recommended [40]. Moreover, the average simulated operative air temperature (25.35 °C) and air speed (0.09 m/s) met the strictest design criteria for offices in the summer season (operative temperature of 24.5 ± 1 °C and maximum air speed of 0.12 m/s) [40].

5. Conclusions

This paper describes the results of a verified and validated CFD model of a highly-glazed meeting room in the Engineering Building at the NUI Galway, Ireland. The comprehensive field measurements performed in the real-life scenario supported CFD model generation and validation. Previously

Please reference as:
Hajdukiewicz, M., Geron, M., & Keane, M.M., 2013. 'Calibrated CFD simulation to evaluate thermal comfort in a highly-glazed naturally ventilated room'. *Building and Environment*, 70, pp. 73-89. http://dx.doi.org/10.1016/j.buildenv.2013.08.020

proposed formal calibration methodology guided towards the creation of the final CFD model that showed a satisfactory agreement with the field measurements.

The following conclusions can be drawn from the study:

- The grid convergence index method for model verification could only be used where the monotonic convergence of the solution was observed. In the case of the divergence of the solution, only qualitative verification was performed.
- The specification of validation criteria based on the purpose of the model (here, thermal comfort requirements) proved to be a clear and straightforward way of validating CFD results with measurements.
- Solar radiation played a significant role in the highly-glazed room, even if only the diffuse part of solar irradiance was considered in the analysis.
- The specification of boundary conditions as the average values over the period monitored was accurate and representative for this period.
- When the complete and detailed boundary conditions are specified in the CFD model and only few assumptions are made in the model boundary conditions, the calibration process can be finalised relatively quickly, generating an accurate representation of the operating environment.
- The parametric analysis may play an effective role in estimating the influence of boundary conditions on model results. In this case study, the parametric analysis established that inlet air speed vertical component influenced air speeds inside the room the most. The indoor air temperatures were mostly influenced by the inlet velocity vertical component, solar radiation through the windows, inlet velocity horizontal component and outdoor air temperature.
- The thermal comfort analysis of the particular scenario confirmed satisfactory and optimal operation of the meeting room in terms of thermal environment. The *PMV*, *PPD* values and local discomfort indices indicated an almost neutral thermal sensation with very low percentage of thermally dissatisfied occupants. The average simulated operative temperature was very close to the optimum value recommended by the standards. Moreover, average simulated operative air temperature and air speed for the particular scenario met the strictest design criteria for offices in the summer season specified in the standards.

In summary, the CFD model calibration methodology bridges the gap between understanding and application of CFD simulation and field measurement for natural ventilation systems. This is done through a systematic utilisation of the best practice guidelines and standards. This study employed the methodology and field measurements in order to develop a 3D CFD model that gives a comprehensive view on environmental conditions in a naturally ventilated highly-glazed office-type meeting room. Furthermore, the validated CFD model and field measurements were used to evaluate thermal comfort indices for the occupants of the meeting room. The satisfactory and optimal operation of the naturally ventilated meeting room for the particular scenario, in terms of thermal environment, has been confirmed. This case study showed that natural ventilation can maintain healthy and

Please reference as:
Hajdukiewicz, M., Geron, M., & Keane, M.M., 2013. 'Calibrated CFD simulation to evaluate thermal comfort in a highly-glazed naturally ventilated room'. *Building and Environment*, 70, pp. 73-89. http://dx.doi.org/10.1016/j.buildenv.2013.08.020

comfortable environmental indoor conditions for the building occupants, while reducing the energy consumed by buildings at the same time.

Acknowledgements

The authors thank Higher Education Authority for the financial support of this research as part of the NEMBES project. The NEMBES project allows for collaboration between the following institutions: Cork Institute of Technology, University College Cork, National University of Ireland Galway, Trinity College Dublin and University College Dublin. The authors would also like to acknowledge the support of Science Foundation Ireland in funding the National Access Program at the Tyndall National Institute and Enterprise Ireland, which have funded aspects of this work.

References

[1] US EPA, “United States Environmental Protection Agency,” 2012. [Online]. Available: http://www.epa.gov/.

[2] European Union, “Official website of the European Union,” 2012. [Online]. Available: http://www.europa.eu.

[3] L. Pérez-Lombard, J. Ortiz, and C. Pout, “A review on buildings energy consumption information,” *Energy and Buildings*, vol. 40, no. 3, pp. 394–398, 2008.

[4] Irish Government, “Building Regulations. Part F: Ventilation,” 2009.

[5] S. Aggerholm, “Perceived barriers to natural ventilation design of office buildings,” 1998.

[6] Arup North America, “Natural ventilation for energy savings in California commercial buildings: Technical potential and barriers project 1,” USA, 2011.

[7] G. Mendes, “Drivers and barriers for natural ventilation in UK,” UK, 2011.

[8] Z. (John) Zhai, M.-H. Johnson, and M. Krarti, “Assessment of natural and hybrid ventilation models in whole-building energy simulations,” *Energy and Buildings*, vol. 43, no. 9, pp. 2251–2261, 2011.

[9] C. C. K. Cheng, K. M. Lam, R. K. K. Yuen, S. M. Lo, and J. Liang, “A study of natural ventilation in a refuge floor,” *Building and Environment*, vol. 42, no. 9, pp. 3322–3332, 2007.

[10] E. A. Hathway, C. J. Noakes, P. A. Sleigh, and L. A. Fletcher, “CFD simulation of airborne pathogen transport due to human activities,” *Building and Environment*, vol. 46, no. 12, pp. 2500–2511, 2011.

[11] T. Catalina, J. Virgone, and F. Kuznik, “Evaluation of thermal comfort using combined CFD and experimentation study in a test room equipped with a cooling ceiling,” *Building and Environment*, vol. 44, no. 8, pp. 1740–1750, 2009.

[12] W.-H. Chiang, C.-Y. Wang, and J.-S. Huang, “Evaluation of cooling ceiling and mechanical ventilation systems on thermal comfort using CFD study in an office for subtropical region,” *Building and Environment*, vol. 48, no. 0, pp. 113–127, 2012.

[13] A. Alajmi and W. El-Amer, “Saving energy by using underfloor-air-distribution (UFAD) system in commercial buildings,” *Energy Conversion and Management*, vol. 51, no. 8, pp. 1637–1642, 2010.

[14] J. Siriwardana, S. K. Halgamuge, T. Scherer, and W. Schott, “Minimizing the thermal impact of computing equipment upgrades in data centers,” *Energy and Buildings*, vol. 50, no. 0, pp. 81–92, 2012.

[15] K.-C. Noh, H.-S. Kim, and M.-D. Oh, “Study on contamination control in a minienvironment inside clean room for yield enhancement based on particle concentration measurement and airflow CFD simulation,” *Building and Environment*, vol. 45, no. 4, pp. 825–831, 2010.

Please reference as:
Hajdukiewicz, M., Geron, M., & Keane, M.M., 2013. ‘Calibrated CFD simulation to evaluate thermal comfort in a highly-glazed naturally ventilated room’. *Building and Environment*, 70, pp. 73-89. http://dx.doi.org/10.1016/j.buildenv.2013.08.020

[16] J. C. Gonçalves, J. J. Costa, A. R. Figueiredo, and A. M. G. Lopes, “CFD modelling of aerodynamic sealing by vertical and horizontal air curtains,” *Energy and Buildings*, vol. 52, no. 0, pp. 153–160, 2012.

[17] AIAA, *Guide for the verification and validation of Computational Fluid Dynamics simulations*. American Institute of Aeronautics and Astronautics, 1998.

[18] U. B. Mehta, “Credible computational fluid dynamics simulations,” *AIAA Journal*, vol. 36, no. 5, pp. 665–667, 1998.

[19] D. Pelletier, “Verification, validation, and uncertainty in Computational Fluids Dynamics,” *Canadian Journal of Civil Engineering*, vol. 37, no. 7, pp. 1003–1013, 2010.

[20] Z. Zhai, Z. Zhang, W. Zhang, and Q. Chen, “Evaluation of various turbulence models in predicting airflow and turbulence in enclosed environments by CFD: Part 1: Summary of prevalent turbulence models,” *HVAC & R Research*, vol. 13, no. 6, pp. 853–870, 2007.

[21] S. Leenknegt, R. Wagemakers, W. Bosschaerts, and D. Saelens, “Numerical sensitivity study of transient surface convection during night cooling,” *Energy and Buildings*, vol. 53, no. 0, pp. 85–95, 2012.

[22] R. Ramponi and B. Blocken, “CFD simulation of cross-ventilation for a generic isolated building: Impact of computational parameters,” *Building and Environment*, vol. 53, no. 0, pp. 34–48, 2012.

[23] M. Hajdukiewicz, M. Geron, and M. M. Keane, “Formal calibration methodology for CFD models of naturally ventilated indoor environments,” *Building and Environment*, vol. 59, no. 0, pp. 290–302, 2013.

[24] P. J. Roache, “Perspective: A method for uniform reporting of grid refinement studies,” *Journal of Fluids Engineering*, vol. 116, no. 3, pp. 405–413, 1994.

[25] ASHRAE, *ASHRAE Handbook - Fundamentals*. Atlanta, USA: American Society of Heating, Refrigerating and Air-Conditioning Engineers, 2005.

[26] NUI Galway, “Engineering Building,” 2012. [Online]. Available: http://www.nuigalway.ie/new-engineering-building/.

[27] Campbell Scientific, “Campbell Scientific, Inc.,” 2011. [Online]. Available: http://www.campbellsci.co.uk/.

[28] IRUSE, “IRUSE weather website,” 2011. [Online]. Available: http://weather.nuigalway.ie/.

[29] R. Everiss, “NUIG Weather App.” Galway, Ireland, 2012.

[30] Onset, “Onset Computer Corporation,” 2011. [Online]. Available: http://www.onsetcomp.com/.

[31] NAP, “National Access Programme,” 2008. [Online]. Available: http://www.tyndall.ie/nap/.

[32] Tyndall, “Tyndall National Institute,” 2012. [Online]. Available: http://www.tyndall.ie/.

[33] B. O’Flynn, S. Bellis, K. Mahmood, M. Morris, G. Duffy, K. Delaney, and C. O’Mathuna, “A 3D miniaturised programmable transceiver,” *Microelectronics International*, vol. 22, no. 2, pp. 8–12, 2005.

[34] FLIR, “Thermal imaging,” 2012. [Online]. Available: http://www.flir.com/IE/.

[35] Ansys, “Ansys, Inc.,” 2012. [Online]. Available: http://www.ansys.com/.

[36] J. Srebric, V. Vukovic, G. He, and X. Yang, “CFD boundary conditions for contaminant dispersion, heat transfer and airflow simulations around human occupants in indoor environments,” *Building and Environment*, vol. 43, no. 3, pp. 294–303, 2008.

[37] I. B. Celik, “Procedure for estimation and reporting of discretization error in CFD applications,” *In Statement on the Control of Numerical Accuracy of the Journal of Fluids Engineering (Editorial Policy), ASME Fluids Engineering Division*, 2008.

[38] L. Eça and M. Hoekstra, “Discretization uncertainty estimation based on a least squares version of the grid convergence index,” 2006.

[39] P. J. Roache, “Error bars for CFD” AIAA 2003–0408, 2003.

Please reference as:
Hajdukiewicz, M., Geron, M., & Keane, M.M., 2013. ‘Calibrated CFD simulation to evaluate thermal comfort in a highly-glazed naturally ventilated room’. *Building and Environment*, 70, pp. 73-89. http://dx.doi.org/10.1016/j.buildenv.2013.08.020

[40] ISO, “ISO 7730: 2005. Ergonomics of the thermal environment - Analytical determination and interpretation of thermal comfort using calculation of the PMV and PPD indices and local thermal comfort criteria,” 2005.

[41] L. G. Berglund and A. P. R. Fobelets, “Subjective human response to low-level air currents and asymmetric radiation,” *ASHRAE Transactions*, vol. 93, no. 1, pp. 497–523, 1987.

[42] MATLAB, “Matlab v.7.12.0.635 (R2011a).” The MathWorks Inc., 2012.

[43] P. O. Fanger, A. K. Melikov, H. Hanzawa, and J. Ring, “Air turbulence and sensation of draught,” *Energy and Buildings*, vol. 12, no. 1, pp. 21–39, 1988.

[44] ANSI/ASHRAE, *Thermal Environmental Conditions for Human Occupancy*. American Society of Heating, Refrigerating and Air-Conditioning Engineers, 2004.

[45] CIBSE, *CIBSE Guide A: Environmental design*, 7th Ed. London, United Kingdom: The Chartered Institution of Building Service Engineers, 2006.

Please reference as:
Hajdukiewicz, M., Geron, M., & Keane, M.M., 2013. ‘Calibrated CFD simulation to evaluate thermal comfort in a highly-glazed naturally ventilated room’. *Building and Environment*, 70, pp. 73-89. http://dx.doi.org/10.1016/j.buildenv.2013.08.020